Enzyme Mechanisms

DOI: 10.1002/ange.201108002

Insights into the Mechanism of the Antibiotic-Synthesizing Enzyme MoeO5 from Crystal Structures of Different Complexes**

Feifei Ren, Tzu-Ping Ko, Xinxin Feng, Chun-Hsiang Huang, Hsiu-Chien Chan, Yumei Hu, Ke Wang, Yanhe Ma, Po-Huang Liang, Andrew H.-J. Wang, Eric Oldfield, and Rey-Ting Guo**

The phosphoglycolipid antibiotic moenomycin directly blocks bacterial cell-wall biosynthesis by inhibiting peptidoglycan glycosyltransferases.[1] The enzyme MoeO5, encoded by the *moe* gene cluster 1 in *Streptomyces ghanaensis*, catalyzes the initial step of moenomycin production, in which the C_{15}-hydrocarbon moiety of farnesyl pyrophosphate (FPP) is transferred to the 2-hydroxy group of 3-phosphoglycerate (3PG), forming an ether bond (Scheme 1).[2] The reaction is similar to that catalyzed by geranylgeranylglyceryl phosphate synthase (GGGPS) for synthesizing archaea-type phospholipids.[3] However, in contrast to the enzyme GGGPS, which gives products with retained all-*trans* configuration of the isoprenyl chain, the enzyme MoeO5 leads to a *trans*-to-*cis* isomerization at the C2=C3 double bond of the transferred farnesyl group.[4] The crystal structures of the proteins GGGPS and the bacterial homologue PcrB reveal a triose-phosphate isomerase (TIM)-barrel fold, which had not been observed previously in prenyltransferases.[3,5] The sequences of GGGPS and PcrB share 35% amino acid identity, but MoeO5 shares only 10% identity with both enzymes (Figure S1 in the Supporting Information). Herein we report the X-ray crystallographic structures of MoeO5 bound to the product 2-(*Z*,*E*)-farnesyl-3-phosphoglycerate (FPG), to the substrate analogue farnesyl thiopyrophosphate (FsPP), and to magnesium (Mg^{2+}) and pyrophosphate (PPi); together with additional biochemical and bioinformatics results, these structures shed light on the possible mechanisms of action of this unusual enzyme.

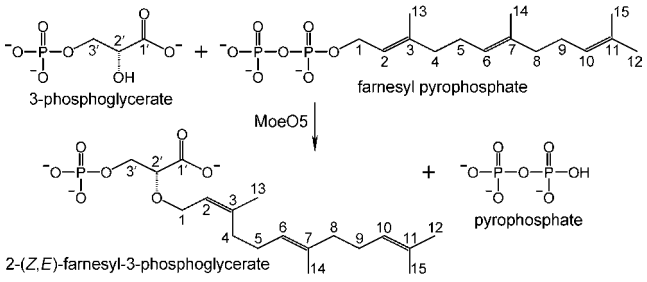

Scheme 1. The first step in moenomycin biosynthesis. The reaction is catalyzed by MoeO5, which transfers the C_{15} farnesyl group from FPP to 3PG. The carbon atoms are numbered 1–15 in FPP and 1′–3′ in 3PG. Importantly, the original all-*trans* configuration is converted to 2-*cis*,6-*trans* (*Z*,*E*) upon the farnesyl transfer, thereby forming 2-(*Z*,*E*)-farnesyl-3-phosphoglycerate (FPG) and pyrophosphate ion (PPi).

Molecular-replacement approaches to determine the structure of MoeO5 by using GGGPS and PcrB as search models were not successful, thereby reflecting perhaps the significant variations in the protein sequences. Because MoeO5 contains no Cys residue, to solve the structure by using multiple isomorphous replacement (MIR), we produced the mutant H97C for efficient preparation of mercury-based MIR derivatives (Table S1 in the Supporting Information). The other structures were solved by molecular replacement (Figure S2 in the Supporting Information and Table 1; see the Supporting Information for details). MoeO5 crystallizes as a homodimer (Figure S3 and Table S2 in the Supporting Information). The dimer interface buries 1200 Å^2, which is more than 10% surface area, on each monomer and mainly involves hydrophobic residues in helices α4 and α5. The *cis*-peptide of Phe140–Pro141 binds to a Mg^{2+} at the molecular dyad (Figure S3 in the Supporting Information). These helices also mediate dimerization in GGGPS and PcrB, but in MoeO5 one of the TIM barrels is rotated by 180° (Figure S4 in the Supporting Information). A more detailed description of the protein structure as well as of the bound ligands can be found in the Supporting Information. Despite its Cα root-mean-square deviation (r.m.s.d.) of about 2.0 Å from the GGGPS and PcrB monomers (Figure S5 in the Supporting Information), the similar protein fold with a connecting loop (denoted λ3) between strands β3 and β4 clearly places MoeO5 among this new class of TIM-barrel prenyltransferases.

The wild-type MoeO5 cocrystallized with a bound product FPG, in which the C_{15} tail moiety makes a U-turn mainly at

[*] F. Ren,[+] Dr. C.-H. Huang, Dr. H.-C. Chan, Y. Hu, Prof. Dr. Y. Ma, Prof. Dr. R.-T. Guo
Industrial Enzymes National Engineering Laboratory
Tianjin Institute of Industrial Biotechnology
Chinese Academy of Sciences, Tianjin 300308 (China)
E-mail: guo_rt@tib.cas.cn

Dr. T.-P. Ko,[+] Prof. Dr. P.-H. Liang, Prof. Dr. A. H.-J. Wang
Institute of Biological Chemistry, Academia Sinica
Taipei 11529 (Taiwan)

X. Feng, Dr. K. Wang, Prof. Dr. E. Oldfield
Department of Chemistry, University of Illinois
Urbana, IL 61801 (USA)
E-mail: eo@chad.scs.uiuc.edu

[+] These authors contributed equally to this work.

[**] This work was supported by the National Basic Research Program of China (grant 2011CB710800 to R.T.G.), Tianjin Municipal Science and Technology Commission (10ZCKFSY06000 to R.T.G.), and the National Institutes of Health (AI074233 to E.O.). We thank the National Synchrotron Radiation Research Center of Taiwan for beam-time allocation and data-collection assistance.

Supporting information for this article is available on the WWW under http://dx.doi.org/10.1002/anie.201108002.

Table 1: Data collection and refinement statistics for the crystals of the native protein MoeO5 and of MoeO5 in the presence of the given reagents. All positive reflections were used in the refinement. Values in parentheses are for the outermost resolution shells.

	Native	FsPP (3 h)	FsPP (overnight)	PPi	3PG
Data collection					
space group	$P2_1$	$P1$	$P1$	$P1$	$P1$
unit-cell					
a [Å]	59.0	46.6	46.7	46.7	46.8
b [Å]	84.5	58.9	58.6	59.7	58.7
c [Å]	59.6	58.8	58.9	59.1	59.2
α [°]	90.0	97.6	97.7	66.7	97.8
β [°]	112.3	108.4	112.2	71.1	112.6
γ [°]	90.0	112.5	108.6	66.0	108.2
resolution [Å]	25–1.39 (1.44–1.39)	25–1.57 (1.63–1.57)	25–1.8 (1.86–1.80)	25–1.66 (1.72–1.66)	25–1.66 (1.72–1.66)
unique reflections	105467 (10291)	70651 (6964)	46862 (4623)	59540 (5880)	59984 (5912)
redundancy	5.1 (5.0)	4.0 (4.0)	4.0 (3.9)	4.0 (4.0)	4.0 (4.0)
completeness [%]	97.5 (95.5)	96.8 (95.1)	96.6 (95.2)	96.1 (94.8)	96.2 (95.0)
average $I/\sigma(I)$	24.8 (3.4)	42.4 (6.4)	37.3 (9.0)	37.1 (9.4)	39.9 (11.4)
R_{merge}[a] [%]	6.9 (55.6)	3.3 (26.6)	3.2 (9.9)	3.1 (9.8)	3.5 (8.6)
Refinement					
no. of reflections	99738 (8573)	69049 (6216)	46545 (4495)	59066 (5627)	59609 (5666)
R_{work}[a] (95% of data)	0.168 (0.222)	0.163 (0.203)	0.161 (0.179)	0.161 (0.184)	0.158 (0.179)
R_{free}[a] (5% of data)	0.189 (0.250)	0.191 (0.243)	0.192 (0.209)	0.186 (0.227)	0.187 (0.220)
r.m.s.d. bonds [Å]	0.020	0.019	0.020	0.020	0.020
r.m.s.d. angles [°]	1.9	1.9	2.0	1.9	2.0
dihedral angles					
most favored [%]	96.2	95.8	95.8	96.2	96.0
allowed [%]	2.6	3.0	3.2	2.8	2.8
disallowed [%]	1.2	1.2	1.0	1.0	1.2
no. of non-H atoms					
protein	3927	3927	3943	3932	3927
water	590	467	405	432	470
ligand	53	53	72	62	59
average B [Å^2][b]					
protein	13.1	18.6	18.0	13.9	14.1
water	26.9	31.6	28.6	26.1	26.4
ligand	12.6	21.2	25.3	17.6	15.8
PDB ID code	3VK5	3VKA	3VKB	3VKC	3VKD

[a] R is the residual difference between the calculated and the observed structure factors (R_{work} and $R_{free}=\Sigma|F_o-F_c|/\Sigma F_o$) or between the measured intensities ($R_{merge}=\Sigma|I_{hj}-I_h|/n\Sigma I_h$, where $j=1-n$, and n is the number of measurements). R_{free} is calculated for 5% randomly selected data which are set aside when the structure is refined against the remaining 95% data. R_{work} is calculated for these 95% data. [b] B is the isotropic temperature of an atom.

the C8=C9 bond (Figure 1), rather than extending straight into a non-polar groove along helix α4 as proposed for GGGPS and PcrB.[3,5] The equivalent groove in MoeO5 is obstructed by the λ3 loop (Figure S6 in the Supporting Information), which contains His97 and is four residues longer than in GGGPS and PcrB (Figure S1 in the Supporting Information).[4] This loop may act as a swinging door for binding and enclosure of the prenyl substrate in GGGPS,[3] but the door is virtually locked up in MoeO5, and the resulting small volume seems barely able to accommodate a C_{10} group. However, substitution of a Tyr residue of GGGPS and PcrB by Ala157 in strand β5 leads to formation of a "nook" for the bent C_{15} group in MoeO5 (Figure S6 in the Supporting Information). Neither the C_{10} geranyl pyrophosphate (GPP) nor the C_{20} geranylgeranyl pyrophosphate (GGPP) is a substrate for MoeO5, and soaking with the *thio*-analogue geranylgeranyl thiopyrophosphate (GGsPP) has no effect on the bound FPG. Clearly the cavity is specific for FPP, and the bent conformation is likely to be important in precisely positioning the C_{15} group for the *trans*-to-*cis* conversion.

On the other hand, the binding site for the 3PG head group is equivalent to that for glycerol 1-phosphate (G1P) in GGGPS (Figure S7 in the Supporting Information).[3] The 3′-phosphate, sandwiched between loop β7–α7 and helix α8′, is fastened by three backbone NH groups (Figure 2a), and the 1′-carboxyl group, together with His97, binds to a water molecule. When the crystals were soaked with FsPP, partial substitution of FPG occurred in three hours, and it was mostly replaced overnight. The β-phosphate group of FsPP occupies the same position as does the 3′-phosphate group of FPG, but the α-phosphate

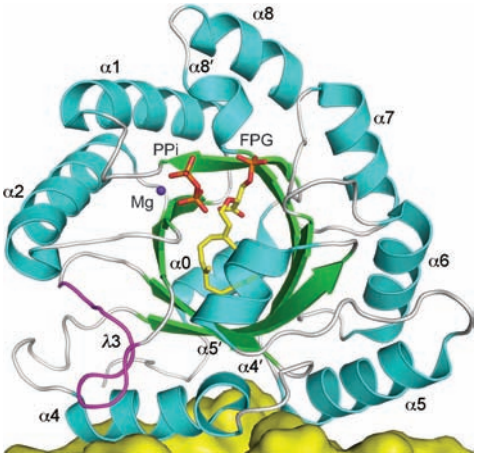

Figure 1. Structure of the MoeO5 monomer. The central eight-stranded β barrel and the surrounding α helices (numbered 0–8) in the ribbon diagram are colored green and cyan, respectively. The unusual loop of λ3 is highlighted in magenta. The bound FPG and Mg–PPi complex (from the crystal soaked with FsPP) are depicted as stick models except Mg^{2+}, which is shown as a blue sphere. A fraction of the other monomer in the MoeO5 dimer is also shown, as a yellow surface presentation.

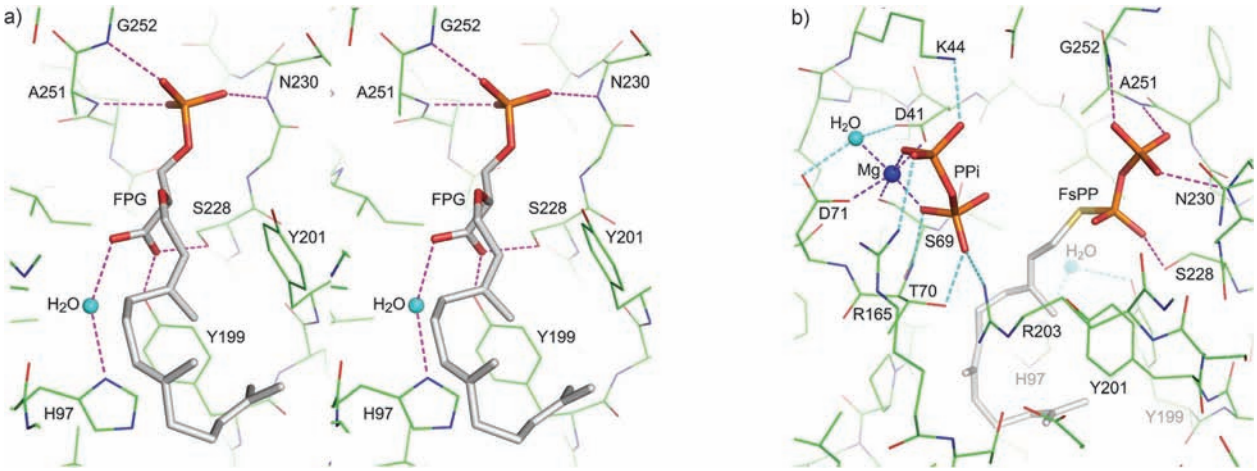

Figure 2. Interactions of MoeO5 with the bound ligands. a) In a stereo view, the FPG is depicted by a thick stick model with gray carbon atoms, red oxygen atoms, and an orange phosphate atom, and the surrounding amino acids are shown as thin sticks with green carbon atoms, red oxygen atoms, and blue nitrogen atoms. Hydrogen bonds between FPG and the protein are shown as dashed lines. The water molecule bound to His97 is consistently observed in all crystals of the wild-type enzyme. b) The bound FsPP and Mg–PPi along with the active-site amino acids are shown in a similar way as in (a) with the sulfur atom in FsPP shown in yellow. The coordinate bonds to the Mg^{2+} and other hydrogen bonds to the ligands are shown as dashed lines. Note that PPi is closer to C1 than to C3 of the FsPP.

group is loosely bound (Figure 2b). Each active site also shows a Mg–PPi complex adjacent to the FsPP, which may represent an alternative disposition of the PPi moiety of FsPP (Figure S8 in the Supporting Information). Here, the Mg^{2+} binds to Asp41, which is highly conserved in MoeO5, GGGPS, and PcrB (Table S3 in the Supporting Information). A similar site containing Mg^{2+} and PO_4^{3-} was found with a 3PG soak, but PPi alone did not bind to this site (details in the Supporting Information). Like most other prenyltransferases, MoeO5 requires Mg^{2+} for activity, and the network of interactions with Mg^{2+} is expected to facilitate FPP ionization, the first step in catalysis.

In the enzymes GGGPS and PcrB, the prenyl carbocation is directly attached to the C3′ hydroxy group of G1P, and the *trans*-configuration is conserved (Scheme 2a). However, for MoeO5 Doud et al. recently proposed catalytic mechanisms in which either nerolidyl pyrophosphate (NPP) was formed after ionization, thereby facilitating bond rotation and the *trans*-to-*cis* conversion (Scheme 2b), or (*Z*,*E*)-FPP was an intermediate.[4] The observation that *trans*-FPP and NPP react at the same rate while *cis*-FPP reacts approximately five times faster (Figure S9 in the Supporting Information) suggests that all three species may be involved. Another possibility is that the His97-bound water molecule, which is 3.6 Å away from the C3 atom, can be activated and associate with the farnesyl cation, thereby transiently forming nerolidol (NOH) and facilitating bond rotation (Scheme 2c). Furthermore, we find

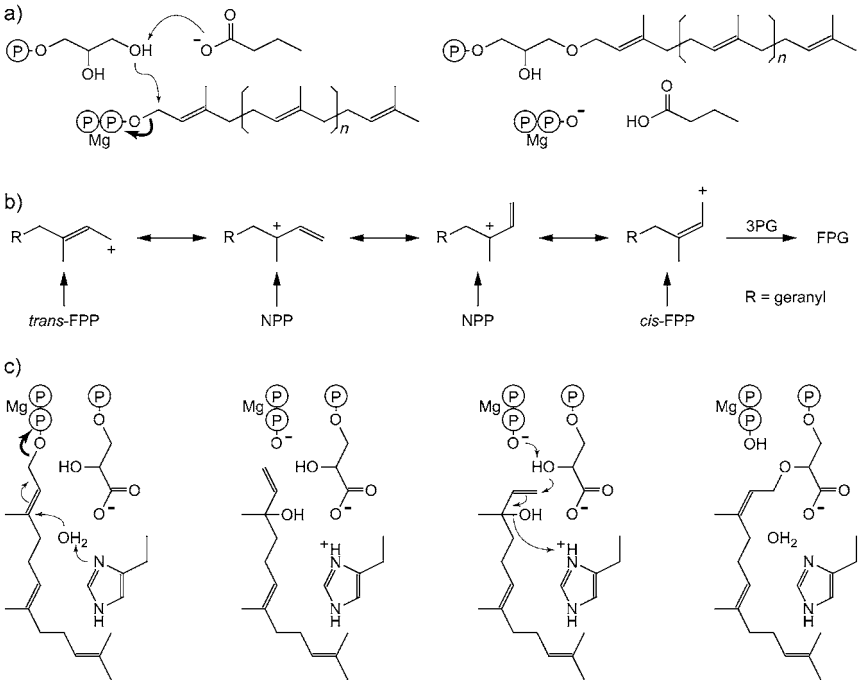

Scheme 2. Proposed mechanisms for the TIM-barrel prenyltransferases. The reactions start by ionization (bold arrow) of the prenyl pyrophosphate, which requires a bound Mg^{2+} ion. a) In catalysis by GGGPS and PcrB, the 3′-OH group of G1P is deprotonated by the Glu167 sidechain (Glu160 in PcrB) and associates directly with the carbocation, forming an ether bond. The prenyl chain length varies from $n=2$ in GGGPS to $n=5$ in PcrB. b) In MoeO5, *trans*-FPP, (*Z*,*E*)-FPP, and NPP all react to form FPG-like products, consistent with an ionization/isomerization mechanism, but shorter and longer chain species do not react to form FPG. c) The residue His97 is essential for catalysis and may play a role in isomerization, possibly via NOH.

that H97C is an inactive mutant, supporting a key role for His97, although (*R*,*S*)-*trans*-NOH (in the presence of 3PG, PPi, and Mg^{2+}) is not a substrate.

In summary, MoeO5 forms a TIM-barrel structure and binds FPG in a curved pocket, mainly as a result of its long λ3 loop. An FPP ionization site containing Asp41 and Mg^{2+} is located nearby, and the results obtained herein are consistent with formation of a (*Z*,*E*)-FPP intermediate. We also find that His97 in the λ3 loop is essential for activity. Except for using Asp41 to bind Mg–PPi, the *cis*-bond formation catalyzed by MoeO5 is distinct from those of other *cis*-prenyltransferases.[6] The crystal structures presented herein thus provide a good starting point for future studies of this novel mechanism of MoeO5 catalysis by using mutagenesis, kinetic analysis, as well as other physicochemical measurements.

Received: November 14, 2011
Revised: January 3, 2012
Published online: March 16, 2012

Keywords: biosynthesis · enzyme catalysis · protein folding · protein structures · prenyltransferases

[1] B. Ostash, S. Walker, *Nat. Prod. Rep.* **2010**, *27*, 1594 – 1617.

[2] a) B. Ostash, A. Saghatelian, S. Walker, *Chem. Biol.* **2007**, *14*, 257 – 267; b) B. Ostash, E. H. Doud, C. Lin, I. Ostash, D. L. Perlstein, S. Fuse, M. Wolpert, D. Kahne, *Biochemistry* **2009**, *48*, 8830 – 8841.

[3] J. Payandeh, M. Fujihashi, W. Gillon, E. F. Pai, *J. Biol. Chem.* **2006**, *281*, 6070 – 6078.

[4] E. H. Doud, D. L. Perlstein, M. Wolpert, D. E. Cane, S. Walker, *J. Am. Chem. Soc.* **2011**, *133*, 1270 – 1273.

[5] a) H. Guldan, F. M. Matysik, M. Bocola, R. Sterner, P. Babinger, *Angew. Chem.* **2011**, *123*, 8338 – 8341; *Angew. Chem. Int. Ed.* **2011**, *50*, 8188 – 8191; b) J. Badger, J. M. Sauder, J. M. Adams, S. Antonysamy, K. Bain, M. G. Bergseid, S. G. Buchanan, M. D. Buchanan, Y. Batiyenko, J. A. Christopher, S. Emtage, A. Eroshkina, I. Feil, E. B. Furlong, K. S. Gajiwala, X. Gao, D. He, J. Hendle, A. Huber, K. Hoda, P. Kearins, C. Kissinger, B. Laubert, H. A. Lewis, J. Lin, K. Loomis, D. Lorimer, G. Louie, M. Maletic, C. D. Marsh, I. Miller, J. Molinari, H. J. Muller-Dieckmann, J. M. Newman, B. W. Noland, B. Pagarigan, F. Park, T. S. Peat, K. W. Post, S. Radojicic, A. Ramos, R. Romero, M. E. Rutter, W. E. Sanderson, K. D. Schwinn, J. Tresser, J. Winhoven, T. A. Wright, L. Wu, J. Xu, T. J. Harris, *Proteins* **2005**, *60*, 787 – 796.

[6] a) R. T. Guo, T. P. Ko, A. P. Chen, C. J. Kuo, A. H. Wang, P. H. Liang, *J. Biol. Chem.* **2005**, *280*, 20762 – 20774; b) P. H. Liang, *Biochemistry* **2009**, *48*, 6562 – 6570.

